Advances in Cryogenic Engineering
Volume 41, pages 1519-1526
1996

SUPERFLUID ORIFICE PULSE TUBE REFRIGERATOR BELOW 1 KELVIN

A. Watanabe, G. W. Swift, and J. G. Brisson[1]

Condensed Matter and Thermal Physics Group
Los Alamos National Laboratory, Los Alamos NM 87545

ABSTRACT

Half the moving parts of the superfluid Stirling refrigerator have been eliminated by adopting an orifice-pulse-tube configuration. Our first such device has cooled to 0.64 K with the hot platform anchored at 1.0 K. Performance of the refrigerator is in reasonable agreement with expectations. Two curious features of the superfluid pulse tube are in distinct contrast with features of conventional pulse tubes. First, stability of the ^{3}He-^{4}He mixture against free convection requires that the hot end of the pulse tube must be *below* the cold end. Second, the low heat capacity of metals below 1 K makes heat loss along the pulse tube due to the fluid's oscillatory motion very small.

INTRODUCTION

The superfluid Stirling refrigerator[2] uses the ^{3}He in a ^{3}He/^{4}He mixture as a thermodynamic working fluid. Bellows-sealed superleak pistons work only on the ^{3}He, carrying it through a Stirling refrigeration cycle. The ^{3}He behaves approximately like an ideal gas; the ^{4}He passes freely through the superleaks, and has little effect on the thermodynamics of the cycle.

In the Stirling refrigeration cycle[3,4], the phasing of the cold piston's motion relative to the oscillating pressure is such that the cold piston absorbs work from the working fluid while the pressure is high, and returns work to the working fluid while the pressure is low; the net effect (averaged over each cycle) is that the cold piston removes work from the fluid. As shown in Fig. 1, in orifice pulse tube refrigerators[5] the cold piston of the Stirling refrigerator is replaced by a passive, dissipative structure which maintains this phasing between fluid flow and pressure in the vicinity of the cold heat exchanger, but with no moving parts. The "orifice" is a resistive flow impedance, which passes oscillatory fluid flow in phase with the oscillatory pressure. Work is thereby removed from the fluid, and dissipated into heat; a heat exchanger near the orifice is thermally anchored to the hot temperature of the refrigerator to dispose of this heat. The "pulse tube" is a simple tube full of the working fluid, connecting the cold heat exchanger to the orifice. It thermally isolates the orifice's dissipation from the cold end, while transmitting fluid motion. In other words, the fluid in the pulse tube can be imagined as a sort of long, thermally insulating piston. The cold end of this imaginary piston, in the vicinity of the cold heat exchanger, mimics the former cold piston of the Stirling

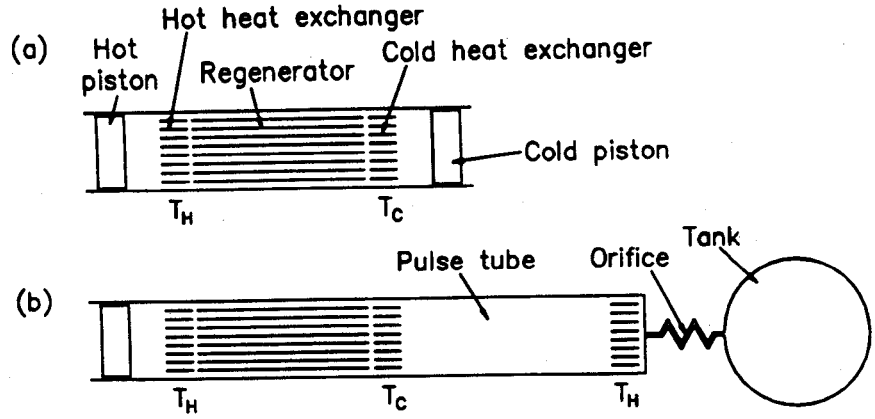

Fig. 1. Schematics of (a) Stirling cycle refrigerator, and (b) orifice pulse tube refrigerator, in which the cold piston of the Stirling cycle refrigerator is replaced by passive components.

refrigerator; the hot end of the imaginary piston delivers net work to the orifice.

In principle, orifice pulse tube refrigerators are less efficient than Stirling refrigerators: Mechanical work is dissipated into heat in the orifice of the pulse tube refrigerator, whereas it is efficiently recovered at the cold piston of the Stirling machine; and the effective thermal conductance of the pulse tube often puts a greater thermal load on the cold heat exchanger than does the heat generated by friction and other losses at the cold piston in the Stirling refrigerator. The lack of cold moving parts is a significant advantage, however, which may outweigh the lower efficiency for some applications. These considerations led us to undertake the work reported here, to explore the application of orifice pulse tube technology to the superfluid Stirling refrigerator. As discussed below, we modified our existing refrigerator, replacing the cold pistons with the simplest possible orifice pulse tube components, and operated it with a 17% mixture. The basic operation of the system is understandable, but a quantitatively accurate understanding will require better knowledge of the thermophysical properties of the mixture. For simplicity, numerical estimates of performance presented here will model the ^{3}He in the mixture using the equation of state and specific heat of a classical ideal gas, and with thermal conductivity $K \sim 0.03$ W/m-K and viscosity $\mu \sim 1.5 \times 10^{-6}$ kg/s-m.

Gravity plays an important role in our pulse tube, both with respect to ordinary convection and by flattening the oscillatory flow profile. Hence ground-based testing will not generally be relevant to the performance of a superfluid pulse-tube refrigerator in zero gravity; a more conventional Stirling configuration of the superfluid Stirling refrigerator may entail less risk for satellite-based applications.

APPARATUS

Our unmodified superfluid Stirling refrigerator, described elsewhere[2] in this volume, essentially comprised two simple Stirling refrigerators as illustrated in Fig. 1a operating thermally in parallel and temporally 180° out of phase from each other. A counterflow heat exchanger served as regenerator, so that the fluid in each of the two refrigerators regenerated that in the other, without need of the usual solid heat capacity.

To convert this apparatus into an orifice pulse tube refrigerator, we removed the two cold pistons, replacing them with two pulse tubes and an orifice as shown in Fig. 2. Because of the 180° temporal phase shift between the two halves of the refrigerator, a single orifice linking the hot ends of the two pulse tubes was used, so that each pulse tube served as the "tank" (cf. Fig. 1b) of the other pulse tube. The heat exchangers at the hot ends of the pulse tubes were thermally anchored to the hot platform.

Choice of dimensions of the pulse tubes was a rough compromise among several considerations. The total fluid volume in the pulse tube should be significantly larger than the volumetric displacement through the pulse tube, so that the "imaginary piston" is not swept entirely out of the pulse tube during operation. The peak-to-peak volumetric displacement of each of our hot pistons was $2V_1 \leq 2$ cm^3, so we expected vol-

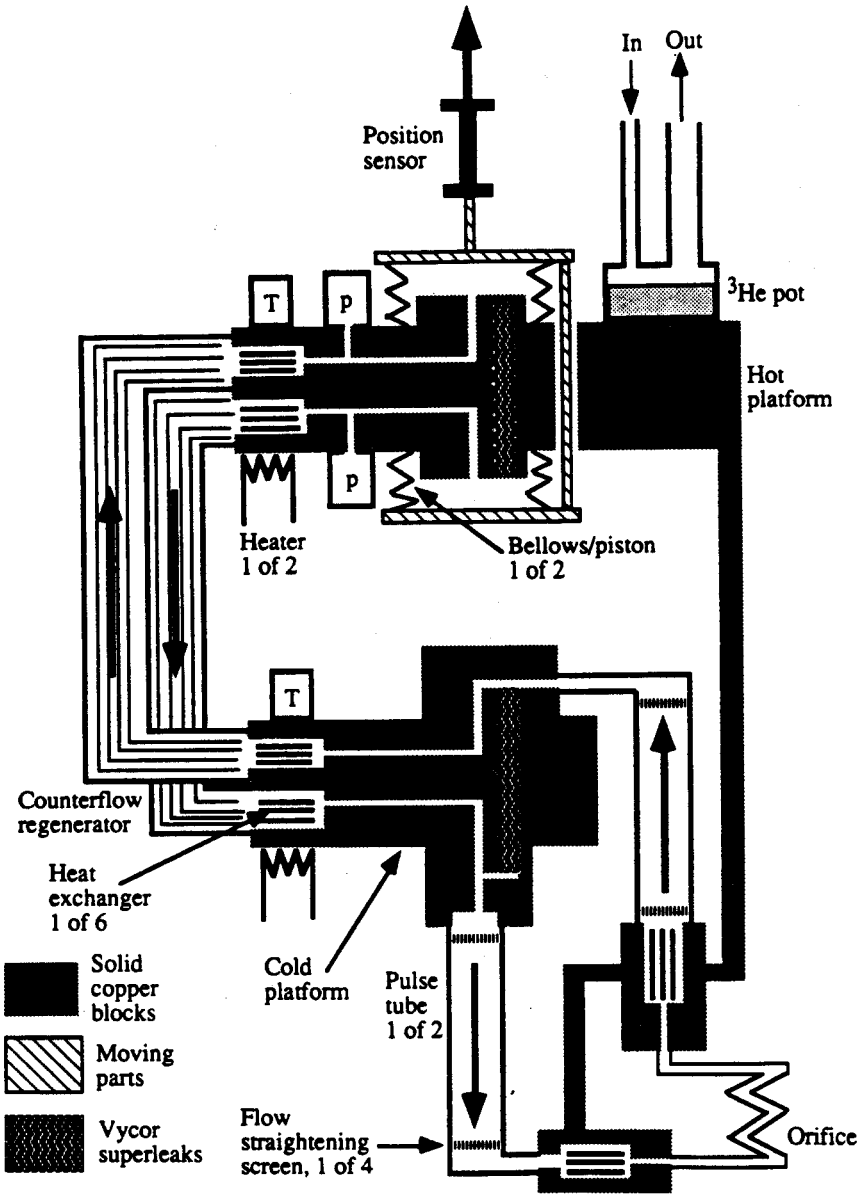

Fig. 2. Schematic of the superfluid orifice pulse tube refrigerator. Pressure sensors are indicated by "p"; thermometers by "T".

umetric displacements in the pulse tubes to be somewhat smaller than that. However, if the pulse tube volume is too large, the pressure amplitude is reduced significantly for a given piston stroke. Erroneously, we had believed that the pulse tube diameter should be significantly larger than the mixture's viscous penetration depth $\delta_\mu = (\mu/\pi f \frac{m*}{m}\rho)^{1/2}$ (where f is operating frequency, ρ is mass of ^{3}He per unit volume, and m^* and m are the effective mass and true mass of a ^{3}He atom), so the "imaginary piston" could move with a velocity that is essentially independent of radial location within the pulse tube. (This consideration will be discussed more fully in the "Gravity" section below.) For the operating frequencies accessible with our drive motor (4 mHz $\lesssim f \lesssim$ 50 mHz), 0.5 mm $\lesssim \delta_\mu \lesssim$ 1.6 mm. The area-to-length ratio of the pulse tube should not be too large, lest ordinary heat conduction along the "imaginary piston" be excessive. Finally, we were constrained by the available space at the bottom of our cryostat. We chose pulse tube inner diameter 6.0 mm and length 7.0 cm, so that the fluid volume in each pulse tube was 2.0 cm^3. The tubes were CuNi with 150 μm thick walls.

Copper screens (60 mesh/inch) at each end of each pulse tube served as flow

straighteners, to prevent possible jetting of fluid entering from the heat exchangers or 3 mm diam connecting tubes, in which the Reynolds number was $\sim 10^3$. The connecting tubes contributed 0.7 cm^3 to the volume of fluid in each half of the refrigerator.

Research orifice pulse tube refrigerators usually use needle valves as orifices so that the impedance can be varied widely during the course of an experiment. For our superfluid orifice pulse tube refrigerator, with small displaced volume and low frequency, the required impedance seemed far higher than the range of commonly available valves. Hence we used a fixed impedance, arrived at by trial and error. It consisted of 16 capillary tubes in parallel, with wires inserted to block most of the area. Each tube was 30 mm long, approximately 0.2 mm inner diameter, with 0.15 mm diameter wire. The Mach number (based on second-sound speed) of the flow in this impedance was ~ 0.01; the Reynolds number was ~ 10.

Each of the hot heat exchangers between the orifice and the pulse tubes was simply four holes (0.8 mm diam, 1 cm long) drilled through a copper block. These blocks were bolted to copper bars, which were in turn bolted to the hot platform.

Thermometers and heaters on the hot and cold platforms allowed measurement of temperatures T and cooling power $\dot{Q}$, and regulation at constant temperature when desired. Piston volumetric displacement V was measured with a variable differential transformer, and oscillatory pressure p was measured with flexible diaphragm sensors. These measurements were automated with a personal computer, so that cycle-averaged work $W = \oint p\,dV$ and average power $\dot{W} = fW$ could be computed easily. More details on these sensors may be found elsewhere.[2]

GROSS COOLING POWER

To investigate basic operation of the refrigerator under simple conditions, we regulated the cold platform temperature T_C to be equal to the hot platform temperature T_H, so that temperature was essentially uniform throughout the apparatus, and measured $V(t)$, $p(t)$, and $\dot{Q}$ as functions of f. The results, shown in Fig. 3, can be understood qualitatively by considering a simple model: an oscillating volume $V(t) = V_0 - V_1\cos(\omega t)$ of gas, weakly linked by a resistive impedance R to a location of constant pressure p_0. (For our dual refrigerator, this location is the midpoint of the orifice.) Viscous pressure drops within V are negligible, so that $p(t)$ is spatially uniform. The mass of gas in the volume is proportional to pV; the rate of change of mass in the volume is $-(p-p_0)/R$. Hence the differential equation describing the system is $d(pV)/dt = -(p-p_0)/R$. Using $p(t) = p_0 + \mathrm{Re}[p_1 e^{i\omega t}]$ and $V(t)$ as given above, we find

$$\frac{p_1}{p_0} = \frac{V_1/V_0}{1 + 1/i\omega R V_0} \quad \text{and} \quad \dot{W} = \frac{p_0}{2R}\left|\frac{p_1}{p_0}\right|^2 . \tag{1}$$

We can easily estimate the parameters in these equations. First, we use $p_0 = 370$ torr, the pressure of a classical ideal gas at 1 K with number density equal to that of a 17% mixture. Second, we use $V_0 = 5.0$ cm^3. The geometrical volume of fluid in each half of the refrigerator is 6.7 cm^3. However, V_0 is somewhat smaller than this, because most of the fluid volume experiences nearly adiabatic pressure oscillations, and hence is stiffer (by a factor $\gamma \sim 5/3$) than we assumed in the isothermal derivation above. Our value of V_0 is based on the estimate that 40% of our geometry should be treated as isothermal and 60% as adiabatic. Finally, we obtain $R = 2.2$ s/cm^3 from the measured 11 s relaxation time of pressure following an abrupt change in piston position.

Using this value of R, the length and number of capillaries, the wire diameters, and the viscosity of the mixture, we estimate that the annular gap between wires and capillaries in the orifice is 7 μm. This is the correct order of magnitude, but a little smaller than would be inferred from the geometry of the capillaries and wires. The flow velocities are of order 10 times the critical velocity for pure ^{4}He in this geometry; perhaps superfluid turbulence plays a significant role in the behavior of the impedance.

With these values for p_0, V_0, and R, Eqs. (1) then yield the lines in Fig. 3, which are in qualitative agreement with the experimental results for the magnitude and phase of p_1 and for $\dot{W}$. (According to Radebaugh's tables[6] for the equation of state, most of the difference between the lines and the measurements is due to our use of the ideal

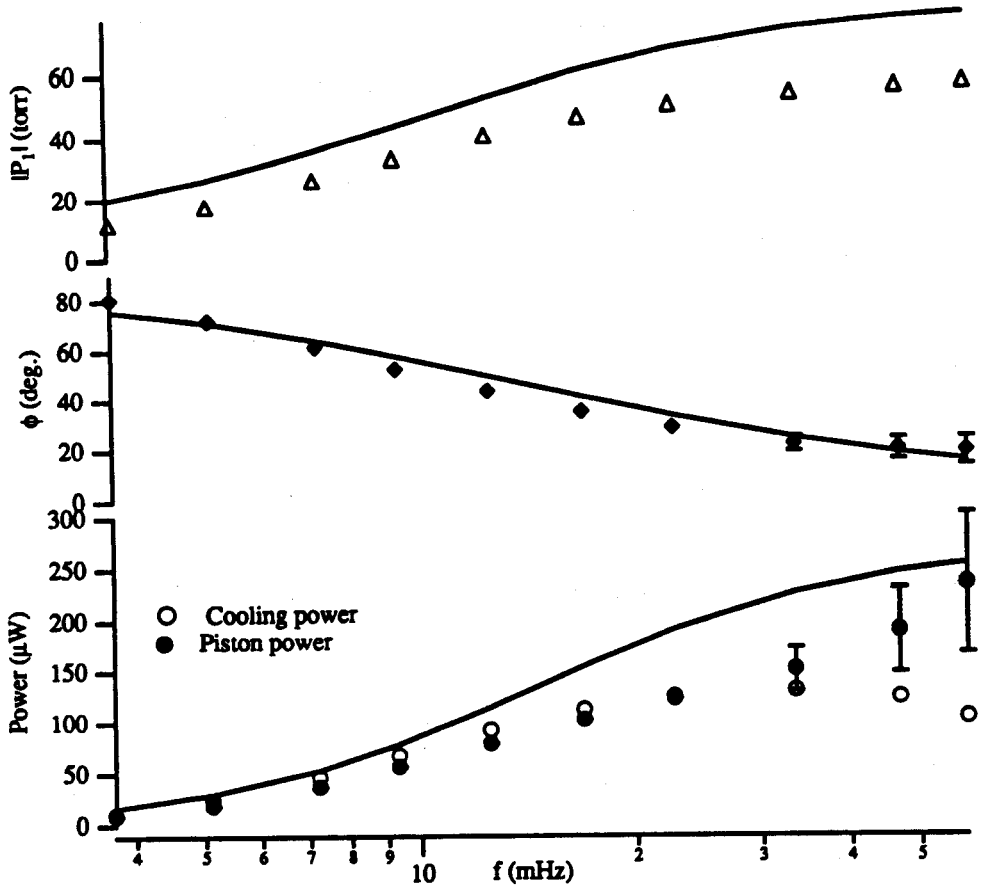

Fig. 3. Amplitude and phase of oscillatory pressure, and cooling power and piston power, vs drive frequency, for $T_C = T_H = 1.0$ K and $V_1 = 0.56$ cm^3. Here, p_1 is the complex amplitude of the pressure difference between the two halves of our refrigerator, and the powers are the sum of those for the two halves, so appropriate factors of 2 have been used relative to Eqs. (1).

gas approximation; but we hesitate to use his values or any others because of the lack of experimental data on osmotic pressure in this concentration range.)

For small regenerator volume and $T_C = T_H$, the volumetric flow rates at the two ends of the regenerator are equal. The work fluxes at the two ends of the regenerator are also equal, because $p(t)$ is spatially uniform. The enthalpy flux through an ideal gas in a perfect regenerator is zero, so the cooling power must equal the time-averaged work flux at the cold end. Hence under these conditions we expect $\dot{Q} = \dot{W}$. At low and mid frequencies, the data agree with this expectation.

We do not fully understand the observed increase of $\dot{W}$ and decrease of $\dot{Q}$ at the highest frequencies. Plausible explanations, in rough agreement with the measurements, include[7] irreversible oscillatory pressure in fluid that is neither isothermal nor adiabatic and nonlinear flow in the impedance.

EFFECTS OF GRAVITY IN THE PULSE TUBE

Initially, we made the mistake of orienting the cold end of the pulse tubes down, following conventional pulse tube refrigerator practice for stability against gravitational convection. With this arrangement, we could not cool below $T_C = 0.95T_H$. Stability against convection in ^{3}He-^{4}He mixtures requires that the cold end be up, because the total (^{3}He + ^{4}He) mass density is lower at the cold end, where the ^{3}He density is higher. To be consistent with our use of the classical ideal gas equation of state for the ^{3}He, we estimate the effective thermal expansion coefficient β_{grav} for purposes of gravitational convection by assuming that the total number density in our mixture of mass-3 and mass-4 atoms is constant, independent of temperature and ^{3}He concentration. Then

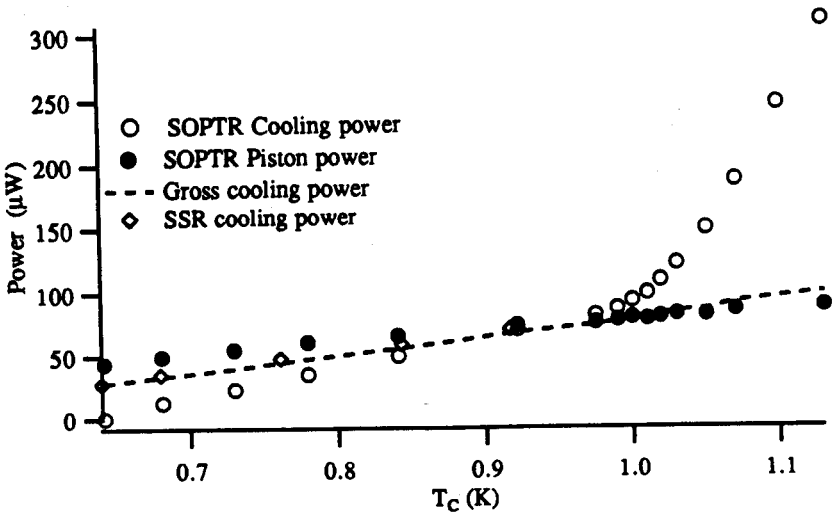

Fig. 4. Powers vs T_C, with $T_H = 1.0$ K and $f = 12.5$ mHz. Circles are measured cooling power and mechanical power with $V_1 = 0.56$ cm^3. Triangles are scaled measured cooling power under similar conditions[2] for conventional Stirling configuration. Dashed line is expected gross cooling power.

it is easy to show that $T\beta_{grav} \cong -1/3$, a third the magnitude and of opposite sign compared to a classical ideal gas. This value is close to tabulations[8] based on a much more complete treatment[9] in the context of Rayleigh-Bènard convection.

All the measurements presented here have the cold end of the pulse tubes up (as shown in Fig. 2). Figure 4 shows typical measurements of cooling power as a function of T_C, with T_H maintained at 1 K. The "cooling power" for $T_C > T_H$ shows a dramatic increase, which we attribute to gravitational convection. For the hottest datum, the Rayleigh number in the pulse tube is of order 10^6.

Gravity also has a profound effect on the oscillatory motion. Consider the x component of the equation of motion of the fluid in the pulse tube:

$$(m^*/m)\rho\left[\partial u/\partial t + (\mathbf{v}\cdot\boldsymbol{\nabla})\,u\right] = -\partial p/\partial x + \mu\nabla^2 u + \rho g_{\rm eff}, \tag{2}$$

where x is directed along the axis of the pulse tube, and is positive downwards, and $g_{\rm eff} = -g/3$ with g the ordinary acceleration of gravity. For small, oscillatory motion, $u \to \mathrm{Re}[u_1(r)e^{i\omega t}]$ and $\rho \to \rho + \mathrm{Re}[\rho_1 e^{i\omega t}]$, so that Eq. (2) reduces to

$$i\omega(m^*/m)\rho u_1 = -\partial p_1/\partial x + \mu\nabla^2 u_1 + \rho_1 g_{\rm eff}. \tag{3}$$

Usually the gravitational term can be neglected. Then the scale of the distance near the walls over which u_1 changes from 0 to its free-stream value is determined by the ratio of the viscous and inertial terms, which yields the (square of the) viscous penetration depth δ_μ alluded to in the introduction. In contrast, in the superfluid pulse tube, we cannot neglect g. The oscillatory displacement of the fluid with its temperature gradient, along the temperature gradient, causes temperature oscillations, contributing a spatially dependent $\rho_1(r)$ proportional to $u_1(r)$. (Density oscillations ρ_1 also arise from pressure oscillations, but these are spatially uniform and so have no effect on the shape of u_1). Then Eq. (3) becomes

$$i\omega(m^*/m)\rho u_1 = -\partial p_1/\partial x + \mu\nabla^2 u_1 - (\rho g_{\rm eff}/T)T_1. \tag{4}$$

with T_1 given by the first-order temperature equation

$$\rho c_p\left[i\omega T_1 + \nabla_x T\, u_1\right] = K\nabla^2 T_1 \tag{5}$$

(again neglecting a spatially uniform term due to pressure oscillations). Combining Eqs. (4) and (5) by eliminating T_1 produces a 4th order differential equation in u_1, whose spatial dependence is governed by an effective viscous penetration depth $\delta_{\mu,\rm eff}$ given in the low-frequency limit by

$$\delta^4_{\mu,\rm eff} = \delta^4_\mu \omega^2 T/4\sigma\,|g_{\rm eff}|\,\nabla_x T, \tag{6}$$

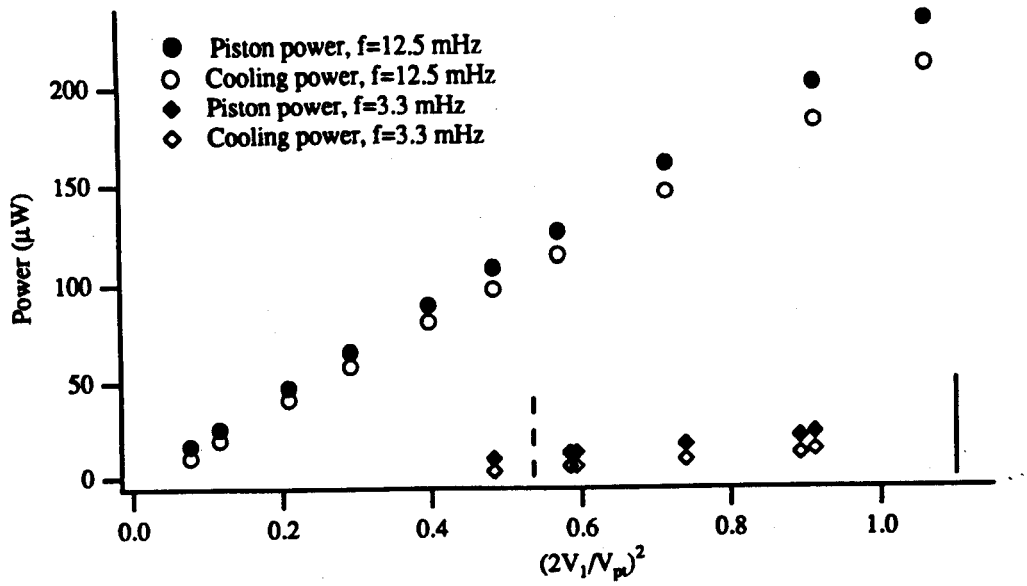

Fig. 5. Cooling power and mechanical power vs piston stroke, with $T_H = 1$ K, $T_C = 0.9$ K, at two different frequencies. Here, we normalize the peak-to-peak piston stroke $2V_1$ by the pulse tube volume $V_{pt} = 2.0$ cm^3, the volume of fluid between the flow straighteners in the pulse tube.

where the Prandtl number $\sigma = \mu c_p/K$. This effective viscous penetration depth gives the scale of the distance near the walls over which u_1 changes from 0 to its free-stream value in our pulse tube. For values appropriate to the data shown in Fig. 4, $\delta_\mu = 0.9$ mm and $\delta_{\mu,\text{eff}} = 0.1$ mm: Gravity flattens the velocity profiles dramatically. We believe this effect is important in *conventional* pulse tubes ($g_{\text{eff}} \to g$) only when $\omega^2 T/4\sigma g\, \nabla_x T \ll 1$. Typical pulse tubes are ~ 10 cm long and have $T_H - T_C \sim T$, implying $f \ll 3$ Hz.

Some indirect evidence of this flattening is shown in Fig. 5, which displays cooling power as a function of piston stroke. We expect that the "imaginary piston" in the pulse tube would disappear for large enough piston strokes, because it would be swept entirely out of the pulse tube as the fluid oscillates, dramatically destroying its thermally insulating quality. The diameter of the "imaginary piston" is approximately equal to the pulse tube diameter minus twice the thickness of the fluid layer held motionless near the pulse tube walls by viscosity[10] ; if gravity could be neglected, this layer would have thickness δ_μ, but the effects of gravity reduce its thickness to $\delta_{\mu,\text{eff}}$. The vertical dashed line in Fig. 5 shows, for $f = 3.3$ mHz, the piston stroke above which the imaginary piston would disappear if δ_μ were the appropriate thickness; the vertical solid line shows the location of this expected transition for $\delta_{\mu,\text{eff}}$ the appropriate thickness. (For $f = 12.5$ mHz, the corresponding lines would be at $(2V_1/V_{pt})^2 = 1.6$ and 2.2, respectively.) The measurements are consistent with the $\delta_{\mu,\text{eff}}$ interpretation (with a heat leak of the order of 10 μW that does not increase dramatically with stroke).

This flattening of the velocity profile increases the viscous dissipation in the pulse tube, because it steepens the velocity gradient near the wall. We estimate this dissipation to be $\lesssim 1$ μW for the conditions of Fig. 4; it varies as $V_1^2 f^{3/2}$.

The flattening of the velocity profile also helps make this an essentially ideal pulse tube. The small value of $\delta_{\mu,\text{eff}}$ compared to the pulse tube diameter makes the "imaginary piston" picture reasonably accurate. The heat capacity in the metal tube wall and the heat capacity in the stationary fluid layer adjacent to the wall are small compared to the heat capacity within the first thermal penetration depth in the moving fluid, so negligible heat is transferred laterally to and from the moving fluid; hence shuttle heat loss is small. The strong stability enforced by gravity and the temperature gradient may suppress streaming-driven convective mixing as well. This leaves ordinary thermal conduction in the x direction as the only significant loss mechanism in this pulse tube.

PULSE TUBE THERMAL LOSS

In the Gross Cooling Power section above, we argued that $\dot{Q} = \dot{W}$ when $T_C = T_H$. For unequal temperatures, the measured cooling power $\dot{Q}$ will be reduced by heat loads to the cold heat exchanger through the regenerator and pulse tube, due both to ordinary conduction and to convection driven by the oscillatory fluid motion. Let us call the cooling power if such heat loads were absent the gross cooling power. For small regenerator volume, the ratio of the volumetric flow rates at the two ends of the regenerator must equal T_C/T_H. Then the ratio of work fluxes at the two ends of the regenerator also equals T_C/T_H, because $p(t)$ is spatially uniform. The enthalpy flux through an ideal gas in a perfect regenerator is zero, so the gross cooling power must equal the time-averaged work flux at the cold end. Hence under these conditions we expect the gross cooling power to be $\dot{W}\,T_C/T_H$, where $\dot{W}$ is the work flux at the hot end, as before. The dashed line in Fig. 4 is this expected gross cooling power.

The difference between the gross and observed cooling powers is the sum of the heat loads due to the regenerator and pulse tube. To estimate what fraction is due to the regenerator, we display in Fig. 4 data taken before[2] we replaced the cold pistons with the pulse tubes, for the same ^{3}He concentration and operating frequency. (To account as well as possible for the slightly different piston stroke used in the earlier data, we multiplied the earlier cooling powers by 0.85 to bring the observed $T_C = T_H$ cooling powers, and hence the gross cooling powers, into agreement.) These data fall much closer to the gross cooling power line than do the data for the pulse tube system, suggesting that the heat load on this system is largely due to the pulse tubes. The data are in rough agreement with our estimate (from geometry and the thermal conductivity of the mixture) that ordinary conduction through the pulse tubes should deliver $(50\ \mu\mathrm{W/K})(T_H - T_C)$. Although many pulse tubes suffer from substantial thermal loss due to streaming- or turbulence-driven mixing, there is no evidence of such loss here.

By using longer, thinner pulse tubes, it will be simple to reduce pulse tube losses by an order of magnitude in future superfluid orifice pulse tube refrigerators, while still keeping $\delta_{\mu,\mathrm{eff}}$ much smaller than the pulse tube diameter and keeping viscous dissipation within $\delta_{\mu,\mathrm{eff}}$ acceptably low. Hence, we expect that a ground-based superfluid pulse tube refrigerator can perform nearly as well as a superfluid Stirling refrigerator, except for the added heat loads imposed on the heat sink at T_H by the orifice dissipation.

ACKNOWLEDGMENT

This research has been supported by the Division of Materials Science in the US Department of Energy's Office of Basic Energy Sciences. We acknowledge helpful conversations with Ray Radebaugh, Mike Hayden, and Bob Ecke.

REFERENCES

1. Permanent address: Mechanical Engineering Department, 41-206, Massachussetts Institute of Technology, 77 Massachusetts Avenue, Cambridge MA 02139.
2. A. Watanabe, G. W. Swift, and J. G. Brisson, Measurements with a recuperative superfluid Stirling refrigerator (1996) elsewhere in this volume; and references therein.
3. G. Walker, "Stirling Engines," Clarendon, Oxford (1960).
4. G. Walker, "Cryocoolers," Plenum, New York (1983).
5. R. Radebaugh, Advances in Cryogenic Engineering 35:1191 (1990).
6. R. Radebaugh, Thermodynamic Properties of ^{3}He-^{4}He Solutions with Applications to the ^{3}He-^{4}He Dilution Refrigerator, National Bureau of Standards Technical Note 362, Boulder CO (1967).
7. A. Watanabe, Studies of superfluid Stirling and pulse tube refrigeration, Master's thesis, Massachusetts Institute of Technology (1995).
8. Y. Maeno, H. Haucke, R. E. Ecke, and J. C. Wheatley, *J. Low Temp. Phys.* 59:305 (1985), Appendix.
9. A. L. Fetter, *Phys. Rev. B* 26:1164 (1982), Eq. (22).
10. Our calculations of the effective diameter of the imaginary piston use the complex Bessel functions of N. Rott, *Z. Angew. Math. Phys.* 20:230 (1969).